Pulmonary Responses of Acute Exposure to Ultrafine Iron Particles in Healthy Adult Rats

Ya-Mei Zhou,[1,2] Cai-Yun Zhong,[1,2] Ian M. Kennedy,[3] Kent E. Pinkerton[1,2]

[1]Center for Health and the Environment, University of California, Davis, California, USA

[2]Center for Comparative Respiratory Biology and Medicine, University of California, Davis, California, USA

[3]Department of Mechanical and Aeronautical Engineering, University of California, Davis, California USA

Received 24 November 2002; revised 18 March 2003; accepted 4 April 2003

ABSTRACT: As critical constituents of ambient particulate matter, transition metals such as iron may play an important role in health outcomes associated with air pollution. The purpose of this study was to determine the respiratory effects of inhaled ultrafine iron particles in rats. Sprague Dawley rats 10–12 weeks of age were exposed by inhalation to iron particles (57 and 90 $\mu g/m^3$, respectively) or filtered air (FA) for 6 h/day for 3 days. The median diameter of particles generated was 72 nm. Exposure to iron particles at a concentration of 90 $\mu g/m^3$ resulted in a significant decrease in total antioxidant power along with a significant induction in ferritin expression, GST activity, and IL-1β levels in lungs compared with lungs of the FA control or of animals exposed to iron particles at 57 $\mu g/m^3$. NFκB–DNA binding activity was elevated 1.3-fold compared with that of control animals following exposure to 90 $\mu g/m^3$ of iron, but this change was not statistically significant. We concluded that inhalation of iron particles leads to oxidative stress associated with a proinflammatory response in a dose-dependent manner. The activation of NFκB may be involved in iron-induced respiratory responses, but further studies are merited.
 Environ Toxicol 18: 227–235, 2003.

Keywords: pulmonary responses; inhalation; iron particles; oxidative stress; ferritin; IL-1β; NFκB

INTRODUCTION

There is growing evidence for the view that exposure to ambient particulate matter (PM) increases cardiopulmonary morbidity and mortality in susceptible subpopulations (Pope et al., 1995; Gamble and Lewis, 1996). Acute as well as long-term exposure to elevated ambient PM has been associated with exacerbation of asthma, decrements in lung function, an increase in chronic respiratory disease, and greater frequency of emergency hospitalization for respiratory and cardiovascular diseases (Schwartz, 1995; Schwartz and Morris, 1995). However, the role of the physicochemical characteristics of ambient PM in causing adverse health effects is poorly understood. It has been speculated that

Correspondence to: Kent E. Pinkerton, Center for Health and the Environment, University of California, One Shields Avenue, Davis, California 95616; e-mail: kepinkerton@ucdavis.edu

Contract grant sponsor: Health Effects Institute.
Contract grant number: 97-8.
Contract grant sponsor: U.S. Environmental Protection Agency STAR.
Contract grant numbers: R826246 and R82799501.
Contract grant sponsor: National Institutes of Environmental Health Science.
Contract grant number: ES-05707.
Contract grant sponsor: Superfund.
Contract grant number: ES-04699.
Published online in Wiley InterScience (www.interscience.wiley.com).
DOI 10.1002/tox.10119

oxidative stress as well as other biological responses associated with transition metals found in PM may be critical in eliciting the adverse effects of PM exposure.

Ambient PM is a complex mixture of particles containing a variety of components including organic compounds, soot, transition metals, sulfates, and nitrates, as well as other trace elements (Cass et al., 2000). It is critical to characterize and identify the toxicity of individual elements of PM to elucidate PM-associated health effects. Iron is a highly ubiquitous element found throughout the environment and is the predominant transition metal present in ambient PM (Hughes et al., 1998). Iron is capable of redox cycling and plays a pivotal role in the formation of extremely reactive hydroxyl radicals (HO·) through the Fenton reaction. Hydroxyl radicals can attack critical macromolecules to cause lipid peroxidation, protein modification, and DNA damage. These reactions may lead to the depletion or alteration of intracellular antioxidants and/or antioxidant enzymatic activity (Halliwell, 1991; Imlay et al., 1998). Oxidative stress occurs when the formation of reactive oxygen species (ROS) overwhelms cellular antioxidant capacity. The occurrence of oxidative stress may also initiate a number of biological events including inflammation and activation of the redox-sensitive nuclear factor–kappa B (NFκB) signaling pathway (Rahman, 2000).

Intratracheal instillation of transition metals including iron, copper, manganese, nickel, and vanadium in rats and/or humans has been shown to induce ROS and acute pulmonary inflammation (Lay et al., 1999; Rice et al., 2001). It has recently been reported that activation of NFκB by PM_{10} in A549 cells occurs via an iron-mediated mechanism (Jimenez, et al., 2000). However, few studies have tested the pulmonary effects of transition metals by inhalation, the essential exposure route for humans to ambient airborne pollutants. For those limited studies that have examined PM-associated transition metals, the average particle masses used for inhalation were found to be unusually high (mg vs. μg; Campen et al., 2001; Fernandez et al., 2002). In the present study a well-controlled and reproducible flame synthesis was used to simulate typical combustion processes and to generate ultrafine iron particles. Exposure by inhalation to two concentrations of iron particles (57 and 90 $\mu g/m^3$) over a period of 3 days was done using healthy adult rats. Potential pulmonary effects were examined by measuring cytotoxicity, ferritin induction, oxidative stress, alteration of proinflammatory cytokines, and activation of the transcription factor NFκB.

Abbreviations

PM	particulate matter
EELS	electron energy loss spectroscopy
XRD	X-ray diffraction
XRF	X-ray fluorescence
BAL	bronchoalveolar lavage
FRAP	ferric reducing/antioxidant power
GSH	glutathione
GSSG	glutathione disulfide
GST	glutathione-S-transferases
EMSA	electrophoretic mobility shift assay

MATERIALS AND METHODS

Chemicals

Acetylene and ethylene were purchased from Airgas (Sacramento, CA). Iron pentacarbonyl, reduced glutathione, glutathione disulfide (GSSG), glutathione reductase, 5,5′-dithio-bis(2-nitrobenzoic) acid (DTNB), 1-chloro-2,4-dinitrobenzene (CDNB), reduced nicotinamide adenine dinucleotide phosphate (NADPH), 2-vinylpyridine, ferrous sulfate, ferric chloride, and tripyridytriazine (TPTZ) were purchased from Sigma-Aldrich (St. Louis, MO).

Particle Generation System

Most practical high-temperature industrial processes use hydrocarbon fuels that are not premixed with air. This form of combustion has been simulated with a laminar diffusion flame system that previously was described in detail (Yang et al., 2001). Briefly, mixtures of acetylene and ethylene were used as fuels; ethylene was the base fuel, and acetylene was added as needed to compensate for the oxidation of soot by iron, which is an effective catalyst of low-temperature carbon oxidation. Iron pentacarbonyl was introduced as a vapor by passing acetylene and ethylene over a liquid iron pentacarbonyl solution. The pentacarbonyl decomposed at a low temperature to yield a source of elemental iron in the flame.

The particle emission from the flame was diluted by filtered air to bring the concentration to two levels that could be maintained for the duration of short-term animal exposure studies. The system was operated to generate minimal soot formation, whereas the iron loading could be varied from 50 to 100 $\mu g/m^3$ in the diluted postflame emission. Particles generated in the system were collected on Teflon filters and 200-mesh holey grids. The morphology and phase of particles collected from the exposure chambers were examined with a Philips EM-400 transmission electron microscope (TEM) operated at 100 kV. Morphology and chemical composition were determined by electron energy loss spectroscopy (EELS) using a JOEL JEM-200CX transmission electron microscope equipped with a Gatan 666 EELS spectrophotometer with a 1.5 eV energy resolution (Yang et al., 2001). X-ray diffraction (XRD) results were obtained on a Scintag XDS 2000 X-ray diffractometer. A differential mobility analyzer was used to measure the size distribution of particles. X-ray fluorescence (XRF) was used to measure the mass concentration of iron particles ($\mu g/m^3$).

Animals

Male Sprague Dawley rats 10–12 weeks of age were purchased from Harlan Laboratories (Indianapolis, IN). All rats were housed in an animal facility with high-efficiency particulate air filters and provided with rat chow and water *ad libitum*. All animals were allowed to acclimate for one week prior to the onset of experimental exposures. Animals were handled in accordance with standards established by the U.S. Animal Welfare Acts as set forth in the National Institutes of Health Guidelines and by the University of California, Davis, Animal Care and Use Committee.

Iron Particle Exposure

Animals were exposed by inhalation in sealed 20 × 43 × 18 cm polycarbonate whole body chambers to two concentrations of iron particles (57 and 90 $\mu g/m^3$) for 3 days, 6 h per day. Three animals were housed in each chamber during exposure. The concentration of iron present in the inhalation chambers was monitored daily by collecting air samples on Teflon filters analyzed by X-ray fluorescence (XRF). Control animals were exposed to filtered air only. Two sets of identical exposures were done for analyses of bronchoalveolar lavage and lung tissues.

Bronchoalveolar Lavage

Bronchoalveolar lavage (BAL) preparation followed Harrod's protocol (Harrod et al., 1998). Briefly, within 2 h following the end of the third day of particle exposure, rats were anesthetized with sodium pentobarbital (Nembutal; Cardinal Health, Inc., Sacramento, CA). The trachea was exposed, cannulated, and secured with a suture. The lungs were lavaged 4 times with a single volume of phosphate-buffered saline (Dulbecco's PBS, Mg^{+2}- and Ca^{+2}-free, pH 7.4; GibcoBRL, Grand Island, NY) at a concentration of 35 mL/kg of body weight. The total cell count for the BAL of each rat was determined using a hemocytometer. Samples containing at least 5×10^4 cells each were spun down in duplicate onto glass slides using a Shandon Model 3 cytospin (Shandon Instruments, Pittsburgh, PA) and stained with Hema 3 (Fisher Scientific Company, Swedesboro, NJ) for determination of the proportion of macrophages, lymphocytes, and neutrophils. A minimum of 500 cells were counted from each cytospin slide.

Total Protein and Lactate Dehydrogenase in BAL

Measurement of the total protein in the BAL supernatant was performed by a modified Bradford assay according to the manufacturer's instructions (BioRad, Hercules, CA), with bovine albumin as the standard. The activity of lactate dehydrogenase (LDH) released from the cytoplasm of damaged cells into the BAL supernatant was measured using a colorimetric assay kit (Sigma-Aldrich, St. Louis, MO).

Preparation of Lung Homogenates and Nuclear Protein Extract

Following iron particle exposure, rats were anesthetized with sodium pentobarbital (Nembutal; Cardinal Health, Inc., Sacramento, CA). The lungs were removed immediately from the thorax and frozen in liquid nitrogen. Lung tissues were subsequently homogenized in ice-cold Tris-HCl buffer (25 m*M* Tris, 1 m*M* EDTA, 10% glycerol, 1 m*M* DTT, pH 7.4) with a glass homogenizer. The homogenate was centrifuged at 10 000 × g for 20 min at 4°C. The resulting supernatant and sediment fractions were separated, and the supernatant was aliquoted and stored at −80°C. The crude nuclear fraction in the pellet was collected and washed three times with homogenate buffer containing Triton X-100, followed by washing one time without Triton X-100. Nuclear protein was extracted with buffer C (20 m*M* HEPES, 25% glycerol, 0.42*M* NaCl, and 1 m*M* EDTA) by centrifuging at 50 000 × g for 30 min. For the glutathione assay, the tissues were homogenized with the addition of 6% metaphosphoric acid. Protein concentrations of lung homogenate and nuclear extract were determined by a modified Bradford assay according to the manufacturer's instructions (BioRad, Hercules, CA), with bovine serum albumin as the standard.

Glutathione

Glutathione (GSH) content of the lung homogenates was measured by an enzymatic method (Tietz, 1969; Anderson, 1985), using a 5,5′-dithio-bis (2-nitrobenzoic) acid (DTNB)–oxidized glutathione reductase recycling assay. Reduced GSH was oxidized by DTNB to give oxidized GSH (GSSG) with the stoichiometric formation of 5-thio-2-nitrobenzoic acid (TNB). GSSG was reduced to GSH by the action of glutathione reductase and NADPH. The rate of TNB formation was measured at 412 nm and was proportional to the sum of the GSH and GSSG present in the sample. GSSG was determined following derivatization with 2-vinylpyridine.

Glutathione-S-Transferases

Glutathione-S-transferase (GST) enzyme activity of lung homogenates was measured spectrophotometrically using the standard substrate, 1-chloro-2,4-dinitrobenzene (CDNB), as previously described (Habig, et al., 1974). The activity was reported as micromoles of CDNB conjugated with GSH per minute per milligram of protein, monitored by the rate change in absorbance at 340 nm at 25°C. The reaction rate was determined by subtracting the background rate of conjugation

in the absence of the enzyme from the rate of conjugation in the presence of the enzyme.

Total Antioxidant Power

Total antioxidant power within lung homogenates was determined by the ferric reducing/antioxidant power (FRAP) assay according to protocol (Benzie and Strain, 1999). At low pH, ferric tripyridytriazine (Fe^{3+}–TPTZ) complex is reduced to the ferrous form and measured by change in absorbance at 593 nm. The change in absorbance is directly related to the total reducing power of electron-donating antioxidants present in the reaction mixture of the biological samples.

ELISA for Proinflammatory Cytokines

The levels of the proinflammatory cytokines IL-1β and TNF-α were assessed in lung homogenates by rat ELISA kits according to the manufacturer's instructions (R&D Systems, Minneapolis, MN). A 1:2 dilution of samples into calibrator diluent provided in the kit was used for cytokine determination. Quantitation of cytokines was normalized to total protein in the sample.

Western Blot Analysis for Ferritin

Western blot analysis was used to measure ferritin levels in the lungs. Lung homogenates were loaded and separated on 12% sodium dodecyl sulfate-polyactylamide gel electrophoresis (SDS-PAGE), followed by transblotting to an ImmunBlot PVDF membrane (BioRad, Hercules, CA). The membrane was blocked by using buffer (150 m*M* NaCl, 10 m*M* Tris-Hcl, 0.1% Tween-20, pH 8.0) with 5% nonfat milk for 1 h at room temperature and subsequently probed with primary antibody against human ferritin (rabbit anti-human ferritin polyclonal antibody; Dako, Carpinteria, CA) at a dilution of 1:1000. Secondary antibody (horse radish peroxidase–linked goat anti-rabbit IgG; Santa Cruz Biotechnology, Inc., Santa Cruz, CA) was added at a 1:3000 dilution. The blots were subsequently developed using an enhanced chemiluminescence detection kit (ECL; AmerSham Pharmacia Biotech, Inc., Piscataway, NJ). Following exposure on autoradiography film, immunoreactive protein bands were quantified by densitometry.

NFκB–DNA Binding Activity

Electrophoretic mobility shift assay (EMSA) was performed to determine NFκB–DNA binding activity. The oligonucleotide used as the probe (Promega, Madison, WI) for EMSA was double-stranded DNA containing an NFκB consensus sequence (5′–CCTGTGCTCCGGGAATTTCCCTGGCC–3′) labeled with [γ-^{32}P]-dATP using T4 polynucleotide kinase. The binding reaction of the nuclear proteins to the probe was assessed by incubation of mixtures containing 5 μg of nuclear protein, 0.5 μg of poly (dI·DC), and 40 000 cpm of γ ^{32}P-labeled probe in the binding buffer (7.5 m*M* HEPES, 35 MM NaCl, 1.5 MM $MgCl_2$, 0.05 m*M* EDTA, 1 m*M* DTT, 7.5% glycerol) for 30 min at 25°C. For the competitive assay, excessive unlabeled oligonucleotides were incubated with proteins prior to the addition of a radiolabeled probe. The protein–DNA binding complex was separated on 5% polyacrylamide gel electrophoresis and autoradiographed overnight.

Statistical Analysis

Data are presented as mean $\pm$ *SE* for 6–8 animals per group. One-way analysis of variance (ANOVA) was performed followed by pairwise comparisons with Fisher's protected least significant difference (PLSD) test. Significance was designated at $p < 0.05$.

RESULTS

Particle Characterization

The average total iron concentrations generated under the two conditions were 57 and 90 $\mu g/m^3$, respectively. For each concentration, daily deviations from the mean were less than 10%. The average particle diameter was 72 nm, with a distribution range of 20–140 nm. Numerous particles possessed the morphologic appearance of distinct polyhedrons as observed by transmission electron microscopy [Fig. 1(a)]. EELS analysis revealed the majority of iron particles generated were iron oxide in composition [Fig. 1(b)]. X-ray diffraction indicated maghemite (γ-Fe_2O_3) was the only phase present in the sample, to within the limits of detection of the instrument. In general, isolated iron particles were found in filter samples, although occasional particles were also found to be associated with a small amount of carbonaceous soot [Fig. 1(c)].

Cytotoxicity Assessments

Inhalation of iron particles at a concentration of 90 $\mu g/m^3$ (compared to exposure to iron at a concentration of 57 $\mu g/m^3$ or to filtered air) was associated with a significant elevation in total protein within the lavage fluid [Fig. 2(a)]. However, no significant elevation in LDH activity was noted in either group exposed to iron [Fig. 2(b)]. Compared with the control group, no significant changes were observed in total cell number, cell viability, or cell differentials in BAL following exposure of animals to either iron concentration (data not shown).

Ferritin

Western blot analysis was used to obtain a quantitative comparison of ferritin in lung tissue following exposure to iron particles (Fig. 3). Exposure to iron particles at 90 $\mu g/m^3$ resulted in a significant increase in intracellular ferritin content compared with control rats (2.5-fold) or with rats exposed to iron at 57 $\mu g/m^3$ (2.3-fold). No significant difference in ferritin levels was noted between control animals and animals exposed to iron at 57 $\mu g/m^3$.

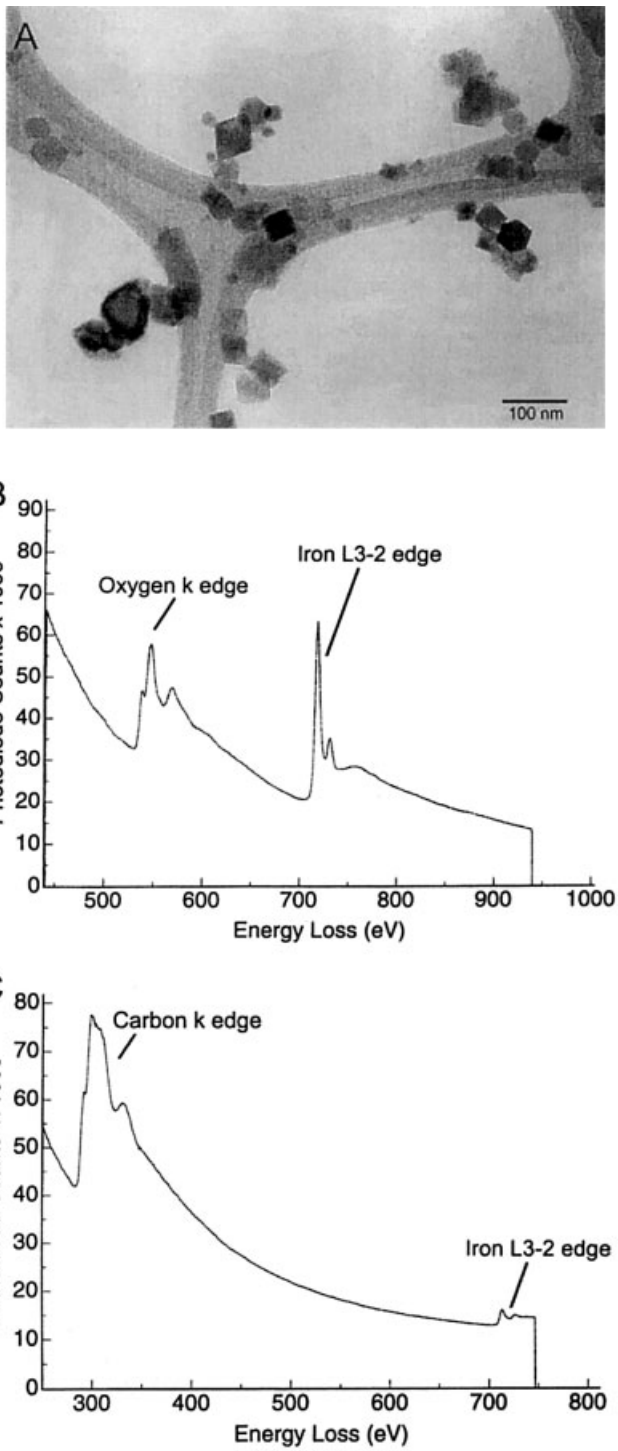

Fig. 1. Ultrafine iron particles generated under diffusion flame conditions. Panel A is a transmission electron micrograph of a holey carbon coated grid containing numerous particles collected from the inhalation exposure unit. The majority of these particles are typically hexagonal or rhomboidal in shape. The scale bar is 100 nm. Panel B is an EELS spectrum obtained from a single particle showing the presence of both oxygen and iron peaks. The ratio of the area under the curve of these particles for iron and oxygen is 0.66, suggesting Fe_2O_3. Panel C is the EELs spectra for a single particle showing only the presence of iron and carbon, but no oxygen. The incidence of this type of particle was dramatically less than for iron oxide particles.

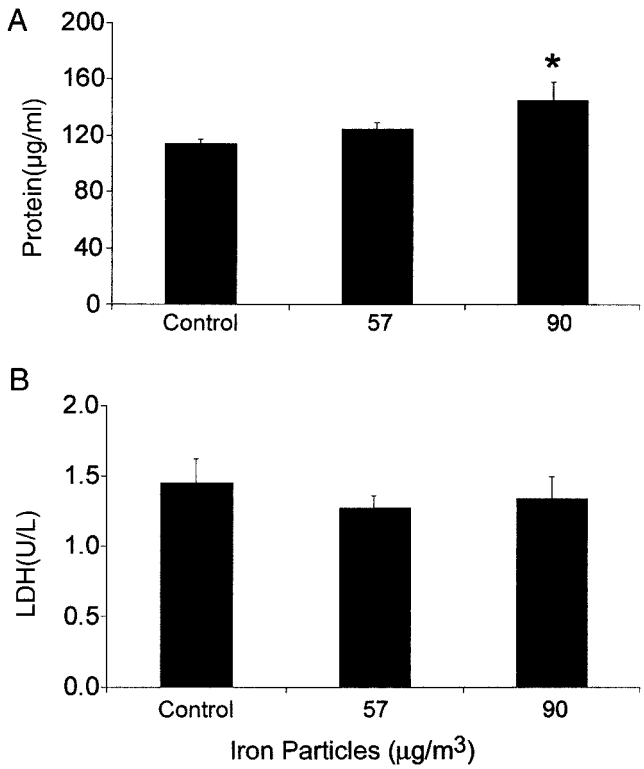

Fig. 2. Effect of iron exposure on protein level (A) and LDH activity (B) in BAL. Values are mean ± SE; n = 8/group. *Significant difference ($P < 0.05$) from control.

Oxidative Stress

Total antioxidant power, GST activity, and intracellular glutathione levels were analyzed in lung tissue homogenates. A statistically significant decrease in total antioxidant power, as indicated by the FRAP value, was noted after exposure to iron particles at 90 $\mu g/m^3$ compared with control animals or animals exposed to iron at 57 $\mu g/m^3$ (Fig. 4). Exposure to iron particles at a concentration of 90 $\mu g/m^3$

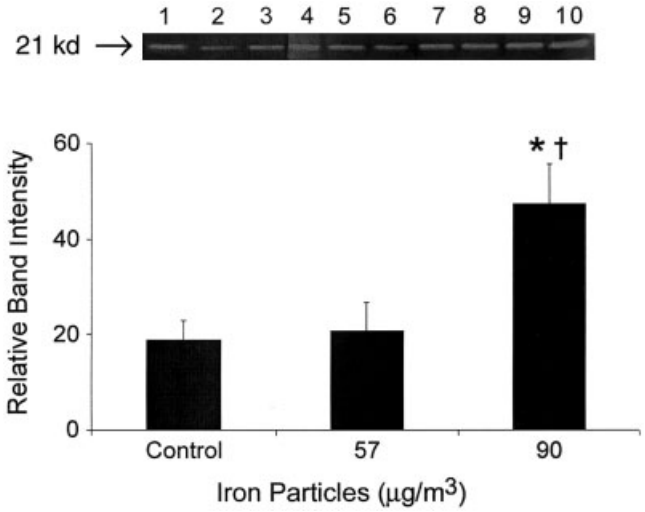

Fig. 3. Effect of iron exposure on intracellular ferritin protein levels in rat lung homogenates. Western blot of 25 g protein from control rats (lanes 1–3), rats exposed to iron at 57 g/m^3 (lanes 4–6) or 90 g/m^3 (lanes 7–9), along with the positive control (lane 10), was separated by 12% SDS-PAGE (upper panel). The band in each lane was positioned at a molecular weight of 21 KD. Quantification of ferritin was analyzed by image densitometry (lower panel). Ferritin content in animals exposed to 90 μg/m^3 of iron was increased 2.5-fold and 2.3-fold over control and animals exposed to 57 μg/m^3 of iron, respectively ($n = 3$). *Significant difference ($P < 0.05$) from control. †Significant difference ($P < 0.05$) from animals exposed to 57 μg/m^3 of iron.

resulted in a significant induction of GST activity compared with control animals and with animals exposed to iron at 57 μg/m^3 (Fig. 5). No significant changes were noted in reduced glutathione (GSH) or in oxidized glutathione (GSSG) following iron exposures (Fig. 6).

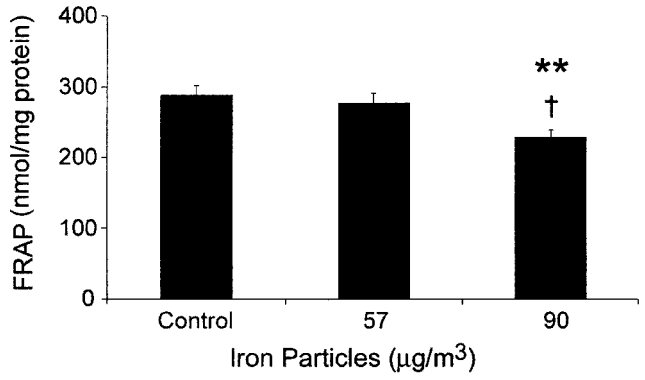

Fig. 4. Effect of iron exposure on total antioxidant power (FRAP value) in lung homogenates. Values are mean ± SE; $n = 8$/group. **Significant difference ($P < 0.01$) from control. †Significant difference ($P < 0.05$) from animals exposed to 57 μg/m^3 of iron.

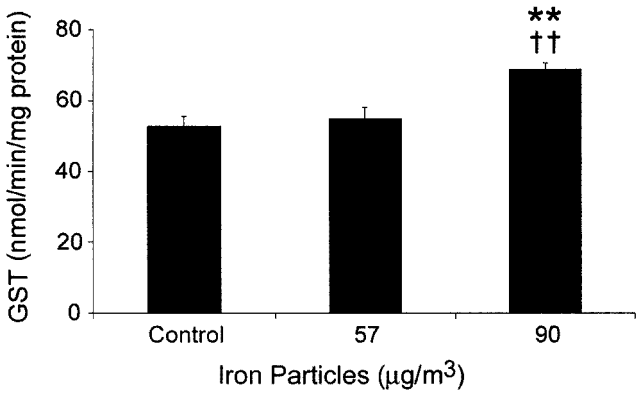

Fig. 5. Effect of iron exposure on GST activity in lung homogenates. Values are mean ± SE; $n = 8$/group. **Significant difference ($P < 0.01$) from control. ††Significant difference ($P < 0.01$) from animals exposed to 57 μg/m^3 of iron.

Proinflammatory Cytokines

Proinflammatory cytokines IL-1β and TNF-α were measured in lung tissue as markers of inflammatory response. IL-1β was significantly increased following exposure to iron at 90 μg/m^3 compared with controls and animals exposed to iron at 57 μg/m^3 [Fig. 7(a)]. No difference was found in TNF-α levels between groups [Fig. 7(b)].

NFκB–DNA Binding Activity

To examine the effects of iron exposure on NFκB activation, EMSA was performed to measure NFκB–DNA binding activity in lung tissue nuclear extract. A 1.3-fold increase in NFκB–DNA binding activity was observed in animals exposed to 90 μg/m^3 of iron compared with control animals (Fig. 8), although this difference was not statistically significant ($p = 0.10$).

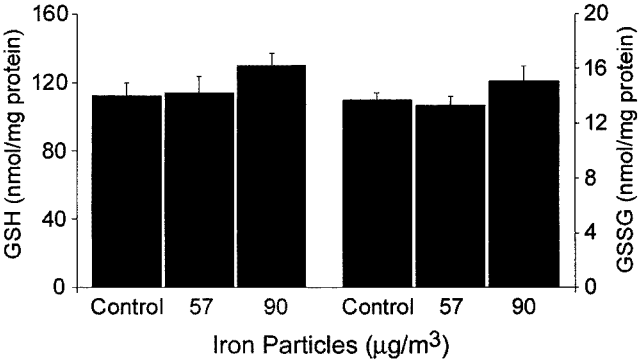

Fig. 6. Comparison of intracellular GSH and GSSG in lung homogenates following iron exposure. Values are mean ± SE; $n = 8$/group.

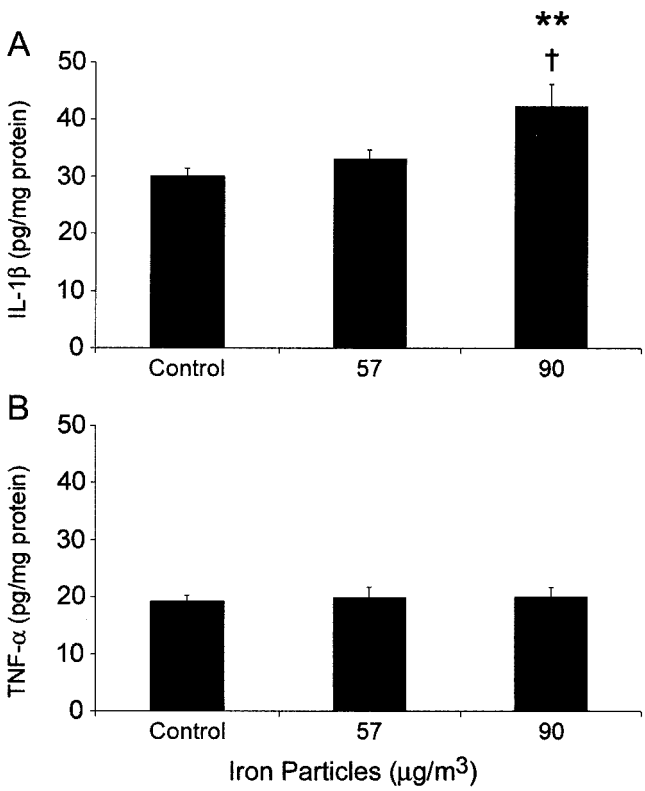

Fig. 7. Effect of iron exposure on the levels of IL-1β (A) and TNF-α (B) in lung homogenates. Values are mean $\pm$ SE; $n = 6$/group. **Significant difference ($P < 0.01$) from control. †Significant difference ($P < 0.05$) from animals exposed to 57 μg/m^3 of iron.

DISCUSSION

A prevailing hypothesis of PM toxicity associates health effects with transition metals present in PM, such as iron, copper, nickel, and vanadium. Studies done *in vitro,* as well as intratracheal instillation of PM, have shown PM-associated transition metals can produce oxidative stress, cytotoxicity, inflammation, and activation of NFκB (Li et al., 1996; Jimenez et al., 2000; Brown et al., 2001; Prahalad et al., 2001). However, when using an inhalation model, the role of individual components in PM to better simulate the natural exposure route of ambient pollutants is largely unknown. Iron was selected because it is the most abundant transition metal found in the environment (Cass et al., 2000). The purpose of this study was to define whether inhalation of iron particles alone could produce adverse respiratory effects in healthy adult rats. Our study demonstrated that exposure to 57 μg/m^3 of iron for 3 days, 6 h per day, did not cause any significant biological responses. Although exposure to iron particles at 90 μg/m^3 did not induce significant cytotoxicity, mild respiratory effects, including significant induction of ferritin as well as elevation in lavage protein and changes in markers of oxidative stress and inflammatory response in the lungs, were noted.

Induction of intracellular ferritin is indicative of bioavailable iron following particle exposure. Increased expression of ferritin has been observed in respiratory epithelial cells treated with iron-containing PM (Fang and Aust, 1997; Smith and Aust, 1997). Ferritin synthesis is known to be regulated by a post-transcriptional mechanism. Bioavailable iron reacts with iron regulatory protein (IRP) to remove the inhibitory protein from ferritin mRNA, allowing the translation of ferritin to proceed (Klausner et al., 1993; Theil, 1994; Harrison and Arosio, 1996). Our study showed that inhalation of iron particles at a concentration of 90 μg/m^3 significantly increased ferritin levels in the lungs. This result suggests that at least part of the iron from these particles deposited in the lungs of rats has become bioavailable. The major form of iron particle generated under our experimental conditions was iron oxide (Fe_2O_3). Iron oxide is considered less toxic and of low bioavailability

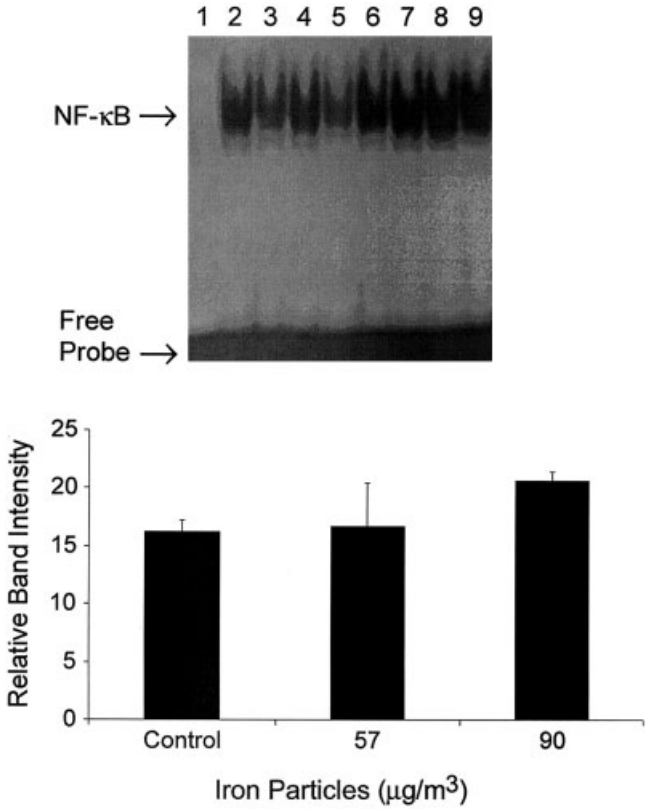

Fig. 8. NFκB-DNA binding activity after iron exposure. Nuclear extracts were prepared with lung tissue and subjected to EMSA for ^{32}P-labeled NF-κB oligonucleotide binding (upper panel). The specificity of NFκB binding activity was tested using 100-fold molar excess of nonlabeled competing NFκB probe to nuclear extract and incubated for 20 min before addition of radiolabeled DNA probe (Lane 1, competition). Lanes 2–4: Control; Lanes 5–6: 57 μg/m^3 of iron; Lanes 7–9: 90 μg/m^3 of iron. Bands were analyzed by densitometry (lower panel). A 1.3-fold elevation of NFκB-DNA binding activity was noted following exposure to ultrafine iron particles at 90 μg/m^3 ($p = 0.10$).

(Stokinger, 1984). We do not anticipate finding that the bioavailable iron in our study resulted from the major forms of iron oxide (Fe_2O_3) present in the aerosol but rather from other forms of iron (for example, iron carbonyl), which account for a small amount of the total iron particles following combustion [Fig. 1(c)]. It is also important to note that the majority of iron particles generated in our study were in the ultrafine range, with an average diameter of 72 nm. Ultrafine particles contribute very little to overall particle mass but dominate in number and surface area in ambient PM samples. Ultrafine particles can be deposited in the most distal parts of the lungs and have direct contact with the surface lining of airways and alveoli to enhance particle transfer to the cell surfaces, with subsequent movement across membranes and uptake into cells (Brown et al., 2000). Taken together, these features may potentiate the iron particles generated in our study to elicit the biological responses observed.

BAL protein and LDH activity both serve as indicators of lung injury and cytotoxicity. Elevation of total protein in BAL indicates increases in microvascular permeability and/or cell lysis, while LDH is an intracellular enzyme whose release implies cell lysis due to toxic events (Axon, et al., 1998). A significant increase in BAL protein content was noted following exposure to 90 $\mu g/m^3$ of iron particles. However, no change was observed in LDH activity following exposure to iron. We speculate that the toxic effects of these inhaled particles may not have been severe enough to cause significant cell lysis, although microvascular leakage may be induced following exposure.

A large body of evidence in recent years has demonstrated that oxidative stress plays an important role in the inflammatory response and the activation of transcription factor NFκB (Rahman, 2000; Rahman and MacNee, 2000). Proinflammatory cytokines such as IL-1β and TNF-α, as well as antioxidant enzymes such as Mn-SOD, γ-GCS, and GST-Pi, are some of the most prominent genes regulated by NFκB (Barnes and Karin, 1997; Hayes and Pulfor, 1995). In this study it was noted that exposure to iron particles at 90 $\mu g/m^3$ was associated with a significant decrease in FRAP and an induction of GST activity, as well as an elevation of IL-1β in the lungs. These changes were accompanied by a slight but statistically insignificant increase in NFκB–DNA binding activity. As a critical antioxidant in the lung, glutathione (GSH) accounts for 90% of intracellular nonprotein thiols and protects cells from oxidative damage (Kelly, 1999; Rahman and MacNee, 1999). A change in GSH redox status such as a decrease in GSH or an increase in GSSG could trigger the synthesis of GSH and may recruit more GSH to target sites from the circulation or other organ systems. It is well established that GSH is maintained at a relatively abundant level in cells (1–10 m*M*) under most physiological conditions (Kelly, 1999; Rahman and MacNee, 2000). In our study significant changes with GSH and GSSG were not observed, suggesting GSH potentially has the capacity to buffer the effects in animals exposed to iron particles, thus minimizing oxidative stress.

In conclusion, the results of the present study have provided the first *in vivo* evidence that iron particles generated through a combustion process can provoke mild, dose-dependent pulmonary effects in healthy adult rats. Because all particles were ultrafine in size and at least a fraction of the iron from these particles became bioavailable, both factors may be responsible for potential mechanisms by which PM-mediated toxicity occurs under the exposure conditions of this study. These findings are the basis for further inquiry into a number of issues associated with health-related PM effects. First, because pulmonary responses in this study were observed following acute, short-term (3-day) inhalation of iron particles, further studies should examine the effects of long-term iron exposure. Such exposures are likely to be more relevant to human exposure to ambient air pollutants. Second, the respiratory effects of iron particles in this study were found in a healthy adult animal model. Because PM-associated health effects in humans are more evident in susceptible subpopulations, these respiratory responses may be more striking and dramatic in a compromised animal model. Third, to further establish the role of transition metals in possible health effects associated with ambient air pollutants, future studies should examine potential interactions between transition metals, such as iron, with other atmospheric pollutants of mixed composition and size, as well as with gaseous air pollutants such as ozone or nitrogen dioxide commonly present in polluted ambient atmospheres.

The authors appreciate the expert technical assistance of Dale Uyeminami and Stephen V. Teague in the generation of exposure conditions and animal care.

REFERENCES

Anderson ME. 1985. Determination of glutathione and glutathione disulfide in biological samples. Methods Enzymol 113:548–555.

Axon RN, Baird MS, Lang JD, Brix AE, Nielsen VG. 1998. Pentalyte decreases lung injury after aortic occlusion-reperfusion. Am J Respir Crit Care Med 157:1982–1990.

Barnes PJ, Karin M. 1997. Nuclear factor–kappa B: a pivotal transcription factor in chronic inflammatory diseases. N Engl J Med 336:1066–1071.

Benzie IFF, Strain JJ. 1999. Ferric reducing/antioxidant power assay: direct measure of total antioxidant activity of biological fluids and modified version for simultaneous measurement of total antioxidant power and ascorbic acid concentration. Methods Enzymol 299:15–27.

Brown DM, Wilson MR, MacNee W, Stone V, Donalson K. 2001. Size-dependent proinflammatory effects of ultrafine polystyrene particles: a role for surface area and oxidative stress in the

enhanced activity of ultrafines. Toxicol Appl Pharmacol 175: 191–199.

Brown LM, Collings N, Harrison RM, Maynard AD, Maynard RL. 2000. Ultrafine particles in the atmosphere: introduction. Phil Trans R Soc Lond A 358:2563–2565.

Campen MJ, Nolan JP, Schladweiler MCJ, Kodavanti UP, Evansky PA, Costa DL, Watkinson WP. 2001. Cardiovascular and thermoregulatory effects of inhaled PM-associated transition metals: a potential interaction between nickel and vanadium sulfate. Toxicol Sci 64:243–252.

Cass GR, Hughes LA, Bhave P, Kleeman, MJ, Allen JO, Salmon LG. 2000. The chemical composition of atmospheric ultrafine particles. Phil Trans R Soc Lond A 358:2582–2592.

Fang R, Aust AE. 1997. Induction of ferritin synthesis in human lung epithelial cells treated with crocidolite asbestos. Arch Biochem Biophys 340:369–375.

Fernandez A, Wendt JO, Cenni R, Young RS, Witten ML. 2002. Resuspension of coal and coal/municipal sewage sludge combustion generated fine particles for inhalation health effects studies. Sci Total Environ 287:265–274.

Gamble JF, Lewis RJ. 1996. Health and respirable particulate (PM10) air pollution: a causal or statistical association? Environ Health Perspect 104:838–850.

Habig WH, Pabst MJ, Jakoby WB. 1974. Glutathoine-S-Transferase: the first step in mercapturic acid formation. J Biol Chem 249:7130–7139.

Halliwell B. 1991. Reactive oxygen species in living systems: source, biochemistry, and role in human disease. Am J Med 91(suppl 3c):145–225.

Harrison PM, Arosio P. 1996. Ferritin: molecular properties, iron storage function and cellular regulation. Biochim Biophys Acta 1275:161–203.

Harrod KS, Mounday AD, Stripp BR, Whitsett JA. 1998. Clara cell secretory protein decreases lung inflammation after acute virus infection. Am J Physiol Lung Cell Mol Physiol 275:L924–L930.

Hayes JD, Pulfor DJ. 1995. The glutathione S-transferase supergene family: regulation of GST and the contribution of the isoenzymes to cancer chemoprotection and drug resistance. Crit Rev Biochem Mol Bio 30:445–600.

Hughes L, Cass G, Gone J, Ames M, Olmez I. 1998. Physical and chemical characterization of atmospheric ultrafine particles in the Los Angeles area. Environ Sci Tech 32:1153–1161.

Imlay JA, Chin SM, Linn S. 1998. Toxic DNA damage by hydrogen peroxide through the Fenton reaction *in vivo* and *in vitro*. Science 240:640–642.

Jimenez LA, Thompson J, Brown DA, Rahman I, Antonicelli F, Duffin R, Drost EM, Hay RT, Donaldson K, MacNee W. 2000. Activation of NF-κB by PM10 occurs via an iron-mediated mechanism in the absence of IκB degradation. Toxicol Appl Pharmacol 166:101–110.

Kelly FJ. 1999. Glutathione: in defense of the lung. Food Chem Toxicol 37:963–966

Klausner RD, Rouault TA, Harford JB. 1993. Regulating the fate of mRNA: the control of cellular iron metabolism. Cell 72:19–28.

Lay JC, Bennett WD, Ghio AJ, Bromberg PA, Costa DL, Kim CS, Koren HS, Delvin RB. 1999. Cellular and biochemical response of the human lung after intrapulmonary instillation of ferric oxide particles. Am J Respir Cell Mol Biol 20:631–642.

Li XY, Gilmour PS, Donaldson K, MacNee W. 1996. Free radical activity and pro-inflammatory effects of particulate air pollution (PM10) *in vivo* and *in vitro*. Thorax 51:1216–1222.

Prahalad AK, Inmon J, Dailey LA, Madden MC, Ghio AJ, Gallagher, JE. 2001. Air pollution particles mediated oxidative DNA base damage in a cell free system and in human airway epithelial cells in relation to particulate metal content and bioreactivity. Chem Res Toxicol 14:879–887.

Pope CA III, Dockery DW, Schwartz J. 1995. Review of epidemiological evidence of health effects of particulate air pollution. Inhal Toxicol 7:1–18.

Rahman I. 2000. Regulation of nuclear factor-κB, activator protein-1, and glutathione levels by tumor necrosis factor-κ and dexamethasone in alveolar epithelial cells. Bio Pharmacol 60: 1041–1049.

Rahman I, MacNee W. 1999. Lung glutathione and oxidative stress: implications in cigarette smoke–induced airway disease. Am J Physiol Lung Cell Mol Physiol 277:L1067–L1088.

Rahman I, MacNee W. 2000. Oxidative stress and regulation of glutathione in lung inflammation. Eur Respir J 16:534–554.

Rice TM, Clarke RW, Godleski JJ, Al-Mutairi E, Jiang N-F, Hauser R, Paulauskis JD. 2001. Differential ability of transition metals to induce pulmonary inflammation. Toxicol Appl Pharmacol 177:46–53.

Schwartz J. 1995. Air pollution and hospital admissions for respiratory disease. Epidemiology 7:21–28.

Schwartz J, Morris R. 1995. Air pollution and hospital admissions for cardiovascular disease in Detroit, Michigan. Am J Epidemiol 142:23–35.

Smith KR, Aust AE. 1997. Mobilization of iron from urban particulates leads to generation of reactive oxygen species *in vitro* and induction of ferritin synthesis in human lung epithelial cells. Chem Res Toxicol 10:828–834.

Stokinger HE. 1984. A review of world literature finds iron oxides noncarcinogens. Am Ind Hyg Assoc J 45:127–133.

Theil EC. 1994. Iron regulatory elements (IREs): a family of mRNA non-coding sequences. Biochem J 304:1–11.

Tietz F. 1969. Enzymatic method for quantitative determination of nanogram amounts of total and oxidized glutathione: application to mammalian blood and other tissues. Anal Biochem 27:502–522.

Yang G-S, Teague S, Pinkerton K, Kennedy IM. 2001. Synthesis of an ultrafine iron and soot aerosol for the evaluation of particle toxicity. Aerosol Sci Tech 35:759–766.